

1 **Electrophysiological characteristics of lead-position-dependent EGM**  
2 **uninterrupted transition during left bundle branch pacing**

3 Jiabo Shen, MD,<sup>1</sup> Longfu Jiang, MD,<sup>1</sup> Hao Wu<sup>1</sup>, Lu Zhang, MD<sup>1</sup>, Hengdong Li MD<sup>1</sup>,  
4 and Lifang Pan<sup>2</sup>

5 <sup>1</sup>Department of Cardiology, Ningbo No.2 Hospital, Ningbo, Zhejiang, China

6 <sup>2</sup>Department of Global Health, Ningbo Institute of Life and Health Industry,  
7 University of Chinese Academy of Sciences, Ningbo, Zhejiang, China

8

9 Address for correspondence:

10 Longfu Jiang, MD

11 Department of Cardiology, Ningbo No.2 Hospital, Ningbo, Zhejiang, China

12 41 Xibei Street

13 Ningbo, Zhejiang, 315010, China

14 Email: longfujianghwamei@163.com

15 Work Telephone Numbers: 86-0574-83871071

16

17 Running title: Characteristics of lead-position-dependent EGM during LBBP

18

19 Word count: 4968

20

21

22

23

24

25

26

27

28

29 **Abstract**

30 **Background and Aims:** Left bundle branch pacing (LBBP) is a novel pacing strategy  
31 that improves ventricular synchrony by utilizing the native conduction system.  
32 However, the current standard practices limit continuous monitoring of paced  
33 electrocardiogram (ECG) and intracardiac electrogram (EGM) transition, which may  
34 result in overlooked or misinterpreted subtle transitions. This study aimed to explore  
35 the electrophysiological characteristics of the lead-position-dependent EGM  
36 continuous transition and evaluate their clinical significance.

37 **Methods:** This observational study included patients referred for LBBP due to  
38 symptomatic bradyarrhythmia. A continuous pacing and recording technique was  
39 employed, allowing real-time monitoring of progressive alterations in the paced QRS  
40 complex as the lead penetrates deeper into the ventricular septum. EGM and ECG  
41 parameters were continuously monitored and analyzed.

42 **Results:** The study encompassed 105 patients, with selective LBBP achieved in 88  
43 patients (83.8%). The amplitude of ventricular EGM predictably changed with radial  
44 interventricular septum depth and peaked in the mid-septum. As the lead was inserted  
45 into the left ventricular subendocardium, the ventricular current of injury (COI)  
46 declined to a level approximating that of the right septum. Continuous recording  
47 technique enabled real-time monitoring of the entire perforation process and the  
48 subtle variations that exist among different perforation modalities. The discernment of  
49 discrete was feasible through the examination of unfiltered EGM, suggesting that  
50 selective LBB capture can also be confirmed by observing the subtle morphological  
51 transitions within the ventricular COI.

52 **Conclusions:** The continuous recording technique provides a more detailed  
53 understanding of the radial depth of the pacing lead throughout the implantation  
54 process. It simplifies the implantation procedures and facilitates the prevention or  
55 early detection of perforations. Future studies are needed to validate these findings  
56 and explore their clinical implications.

57

58 **Keywords:** Left bundle branch pacing; Continuous recording technique; Unfiltered  
59 unipolar electrogram; Current of Injury; Septal perforation.

60

61 **What's new?**

62 1.Utilization of Ventricular Electrogram (EGM) for Lead Positioning: The amplitude  
63 of ventricular EGM changes predictably with radial interventricular septum depth,  
64 peaking in the mid-septum. This provides a useful way to determine whether the lead  
65 is located on the left, right, or middle of the ventricular septum.

66

67 2.Real-time Monitoring of Perforation Process: The continuous recording technique  
68 enables real-time monitoring of the entire perforation process. This feature helps to  
69 distinguish the subtle variations that exist among different perforation modalities,  
70 facilitating early detection and prevention of perforations.

71

72 3.Confirmation of Selective Left Bundle Branch Pacing (SLBBP): The emergence of  
73 a discrete ventricular current of injury (COI) may serve as a novel characteristic of  
74 SLBBP. This suggests that SLBBP can be confirmed by observing the subtle  
75 morphological transitions within the ventricular COI.

76

77 **Introduction**

78 Left bundle branch pacing (LBBP), a novel pacing strategy, utilizes the native  
79 conduction system to improve ventricular synchrony, providing stable pacing  
80 parameters.[1] For the achievement of left conduction system capture, the LBBP lead  
81 must be embedded sufficiently deep within the left ventricular septum's  
82 subendocardium.[2] Current standard practices of intermittent recording technique  
83 require the employment of an alligator clip for lead connection, a link disrupted  
84 during lead rotation, thereby inhibiting the capacity for continuous monitoring of

85 paced QRS transition. Consequently, this may result in overlooked or misinterpreted  
86 subtle transitions. This limitation impedes the precise determination of left bundle  
87 branch (LBB) capture and any changes in the pacing modality as the lead advances  
88 into the ventricular septum.[3, 4] We have previously described a real-time recording  
89 technique that yields improved electrocardiogram (ECG) and intracardiac electrogram  
90 (EGM) recording capabilities in LBBP [5-7]. While previous studies have  
91 comprehensively described the lead-position-dependent QRS transition and  
92 output-dependent QRS and EGM transition,[7-10] the lead-position-dependent EGM  
93 transition remains inadequately established. Therefore, this study aims to explore the  
94 electrophysiological characteristics of the lead-position-dependent EGM continuous  
95 transition and evaluate their clinical significance.

96

## 97 **Methods**

### 98 **Study population**

99 This observational study encompassed consecutive patients referred to our center for  
100 LBBP, due to symptomatic bradyarrhythmia, from September 2022 through  
101 November 2023. Patients for whom definitive LBB capture could not be confirmed  
102 were excluded from the study. The research protocol was approved by the  
103 Institutional Review Board of Ningbo No.2 Hospital, and informed consent was duly  
104 obtained from each participant.

105

### 106 **Definitions of LBB capture**

107 Dynamic paced QRS transition served as a criterion for LBB capture diagnosis.[7, 11,  
108 12] LBB capture is confirmed by paced QRS morphology of the right bundle branch  
109 block pattern and all of the following strict criteria: (1) demonstration of the left  
110 ventricular septal pacing (LVSP) to nonselective LBBP (NSLBBP) transition during  
111 the process of lead screwing and/or NSLBBP to selective LBBP (SLBBP) transition  
112 during unipolar pacing threshold testing, and (2) both low and high outputs

113 maintained the shortest and constant pacing stimulus to V6 R-wave peak time  
114 (Stim-V6RWPT).

115

### 116 **Implantation procedure**

117 This study employs a continuous pacing and recording technique, utilizing a  
118 transseptal pacing lead as detailed in previous researches.[5, 7] Following a  
119 successful puncture of either the left axillary or subclavian vein, the C315 His sheath  
120 (Medtronic, Minneapolis, MN) is positioned in the right ventricle. Angiography is  
121 performed using 30° right anterior oblique fluoroscopy to visualize the tricuspid valve  
122 annulus (TVA), the image of which serves as a reference for the lead implantation site  
123 (**Figure 1A**).[13] Throughout the lead deployment process, a continuous  
124 pacemapping technique is adopted, establishing a persistent connection between the  
125 pacing lead and the pacing system analyzer (PSA) via the John Jiang connecting cable  
126 (Xinwell Medical Technology Co, Ningbo, Zhejiang, China).[5] In contrast to the  
127 interrupted pacing method, in which the alligator cable is momentarily disconnected  
128 during lead rotation, this strategy enables the real-time monitoring of progressive  
129 alterations in the paced QRS complex as the lead penetrates deeper into the  
130 interventricular septum (IVS).

131 The lead implantation procedure and schematic diagrams of the connection have been  
132 presented in earlier studies, illustrated through video documentation.[5, 7] The  
133 operational principle of the John Jiang connecting cable resembles a bearing,  
134 facilitating the free movement of internal and external components. This design  
135 ensures uninterrupted electrical conduction during lead rotation, thereby enabling  
136 continuous pacing and recording of ECG and EGM. The intricate internal structure  
137 and functional mechanism of the connector have been described in a previous study.[5]  
138 The distal pin of the 3830 lead (Medtronic, Minneapolis, MN) is inserted into the  
139 rotatable interface hole of the connector, after which the lead's helix is inserted into  
140 the C315 His sheath and advanced into the right ventricle. Under fluoroscopic

141 guidance, the 3830 lead is positioned at the LBB screw-in site, and the lead body is  
142 then rotated, gradually driving the helix from the right side of the ventricular septum  
143 to the left (**Figure 1B and C**). During this process, careful monitoring of changes in  
144 the ECG and EGM is crucial to accurately identify lead positioning and prevent  
145 perforation. The depth of the lead within the IVS is assessed by contrast injection  
146 from the sheath using a 45° left anterior oblique fluoroscopic view (**Figure 1D-F**).

147

### 148 **Electrophysiological observations**

149 Continuous monitoring of ECG and EGM was conducted using the Workmate Claris  
150 (Abbott, Plymouth, MN) electrophysiology system at a speed of 100 mm/s. A filtered  
151 unipolar ventricular electrogram was obtained with high- and low-pass filter settings  
152 of 200 and 500 Hz to monitor the discrete EGM transition.[14] Unfiltered ventricular  
153 current of injury (COI) was monitored from the tip lead with band-pass filter settings  
154 of 0.5 and 500 Hz using a unipolar configuration during lead rotation.[15] The  
155 ventricular COI manifests as an increase in the duration and elevation of the  
156 ventricular electrogram compared to the baseline (**Figure 2**). Employing a continuous  
157 recording technique allows for the monitoring of changes in electrophysiological  
158 characteristics across all pacing modes during interventricular septum traversal. A  
159 detailed examination was conducted on five representative pacing modes within this  
160 study. Right ventricular septal pacing (RVSP) was defined when the lead was located  
161 in the RVS and exhibited the classic W pattern in lead V1. Intraventricular septal  
162 pacing (IVSP) was defined when the lead was screwed into the ventricular septum,  
163 and QRS morphological changes transitioned from the W pattern to the Qr pattern in  
164 lead V1. LVSP was defined when the lead was screwed into the deep septum,  
165 demonstrating a right bundle branch block pattern just before LBB capture. NSLBBP  
166 was defined when the Stim-V6RWPT for two adjacent paced complexes decreased by  
167 at least 10 ms with a constant output (2 V/0.5 ms) during screwing in. SLBBP was  
168 confirmed when the QRS morphology changed, the Stim-V6RWPT was fixed, and an

169 isoelectric interval and discrete component appeared on the EGM (**Figure 3**).  
170 Measurements, including the maximum amplitude of ventricular COI elevation and  
171 other parameters, were performed by two individuals who were blinded to the study  
172 protocol. The values obtained from these measurements were subsequently averaged  
173 (**Figure 4**). In the event of identifying a perforation, characterized by a positive  
174 ventricular COI transition to a negative ventricular electrogram and high output loss  
175 capture, the lead was carefully withdrawn (**Figure 5**). During this withdrawal process,  
176 unipolar electrograms were continuously monitored to observe the recovery of  
177 positive ventricular COI. This observation served as a confirmation of the perforation.  
178

### 179 **Statistical analysis**

180 Continuous variables are represented as the mean  $\pm$  standard deviation, while  
181 categorical variables are expressed in percentages. Statistical evaluation of differences  
182 among the ECG parameters within the six pacing modalities was conducted using  
183 repeated-measures analysis of variance complemented with Bonferroni post hoc  
184 analysis. A *p*-value of less than 0.05 was designated as the threshold for statistical  
185 significance. Statistical analyses were carried out utilizing SPSS (version 25.0; IBM  
186 Corp., Armonk, NY, USA) and GraphPad Prism 9 (GraphPad Software, Inc., San  
187 Diego, CA, USA).

188

## 189 **Results**

### 190 **Baseline characteristics**

191 This study encompassed a total of 105 patients who underwent pacemaker  
192 implantation. NSLBBP was confirmed in ninety-four patients (89.5%) who displayed  
193 an abrupt shortening of Stim-V6RWPT by at least 10 ms. SLBBP was achieved in 88  
194 patients (83.8%), as indicated by isoelectric intervals and discrete components during  
195 threshold testing. In the absence of a Stim-V6RWPT's abrupt shortening of 10 ms and  
196 an isoelectric interval, LVSP was confirmed in eleven patients.

197 An analysis was performed on paced parameter changes in the 88 patients who met  
198 the criteria for selective LBB (SLBB) capture. The mean age of the patients was 73.7  
199  $\pm$  9.1 years. The left ventricular ejection fraction was reported as 62.8  $\pm$  11.1%. The  
200 indications for pacemaker implantation included atrioventricular block in 56 patients  
201 and sick sinus syndrome in 31 patients. In the pacemaker population, hypertension  
202 was identified in 53 patients, diabetes mellitus in 23 patients, cardiomyopathy in 4  
203 patients, coronary heart disease in 14 patients, and atrial fibrillation in 22 patients.  
204 **Table 1** provides a summary of the patients' characteristics. The pacing-related and  
205 procedure-related characteristics are presented in **Table 2**.

206

### 207 **Lead-position-dependent parameters during implantation**

208 The ECG and EGM parameters at the depth of implantation are documented in **Table**  
209 **3** and **Figure 3**. The ventricular COI amplitude was recorded as 10.5  $\pm$  5.9 mV in the  
210 RVSP group and 11.9  $\pm$  6.4 mV in the SLBBP group, with no significant difference ( $p$   
211 = 0.328). There was no significant difference in the ventricular COI amplitude  
212 between the LVSP and NSLBBP groups (19.8  $\pm$  9.6 mV vs. 20.0  $\pm$  9.2 mV). A  
213 significant statistical difference was observed in the amplitude of ventricular COI  
214 among other pacing modes at varying depths.

215 Impedance was measured as 948.7  $\pm$  202.1 $\Omega$  in the RVSP group and 980.3  $\pm$  156.3  $\Omega$   
216 in the IVSP group, with no significant difference ( $p$  = 0.555). A significant difference  
217 in impedance was noted between the IVSP group (980.3  $\pm$  156.3  $\Omega$ ) and the NSLBBP  
218 group (929.5  $\pm$  191.4  $\Omega$ ) ( $p$  < 0.05), as well as between the NSLBBP group (929.5  $\pm$   
219 191.4  $\Omega$ ) and the SLBBP group (886.0  $\pm$  164.4  $\Omega$ ) ( $p$  < 0.05).

220 Stim-V6RWPT was 103.2 $\pm$ 16.9 ms in the RVSP group and 83.8  $\pm$  12.5 ms in the  
221 IVSP group, with a significant difference ( $p$  < 0.05). There was no significant  
222 difference in Stim-V6RWPT between the IVSP and LVSP groups (83.8  $\pm$ 12.5 ms vs.  
223 81.8 $\pm$ 12.3 ms). However, Stim-V6RWPT significantly shortened from LVSP to



224 NSLBBP ( $67.5 \pm 9.7$  ms,  $p < 0.05$ ), with no significant difference between the  
225 NSLBBP and SLBBP groups ( $66.9 \pm 9.5$  ms).

226 Significant statistical differences were observed in stimulus to V1 R-wave peak time  
227 with different depth pacing modes. No significant difference was noted in  
228 stimulus-QRS end duration (Stim-QRSend) between the LVSP and NSLBBP groups  
229 ( $138.6 \pm 14.3$ ms vs.  $136.0 \pm 18.8$  ms). However, a significant difference in  
230 Stim-QRSend was observed between the NSLBBP group ( $136.0 \pm 18.8$  ms) and the  
231 SLBBP group ( $147.5 \pm 17.6$  ms) ( $p < 0.05$ ).

232 Apart from LVS perforation experienced by three patients, no other procedure-related  
233 complications, such as electrode displacement, pericardial effusion, infection, or  
234 pocket hematoma, were reported.

235

## 236 **Discussion**

237 Our study demonstrates several novel findings: 1) The amplitude of ventricular EGM  
238 predictably changes with radial IVS depth, and peaks in the mid-interventricular  
239 septum, making it a useful ventricular COI feature to distinguish whether the lead is  
240 located on the left, right, or middle of the ventricular septum; 2) As the lead is  
241 inserted into the left ventricular subendocardium, producing a decline in the  
242 ventricular COI to a level approximating that of the right septum, the operation  
243 necessitates an extraordinarily cautious screwing of the lead. Simultaneously, careful  
244 observation of the QRS transition is necessitated along with the execution of output  
245 testing; 3) Continuous recording technique enables real-time monitoring of the entire  
246 perforation process. This feature helps to distinguish the subtle variations that exist  
247 among different perforation modalities; 4) The discernment of discrete is feasible  
248 through the examination of unfiltered EGM. This suggests that SLBB capture can also  
249 be confirmed by meticulously observing the subtle morphological transitions within  
250 the ventricular COI.

251

252 **Mid-interventricular septal pacing**

253 During the implantation procedure of cardiac devices, acute tissue injury, also known  
254 as the COI, can be caused by the fixation of leads into the myocardial tissue. The  
255 presence of COI has been associated with improved acute performance and long-term  
256 stability of active fixation leads.[16-18] It is generally accepted that a deeper  
257 electrode screw-in leads to increased tissue damage, consequently resulting in higher  
258 COI amplitudes. Intriguingly, our study reveals that while deeper electrode insertion  
259 may potentially cause increased myocardial damage, it is not positively correlated  
260 with COI elevation. Instead, it exhibits an inverted U-shaped relationship, resembling  
261 a parabolic curve. This suggests that the injury current might be associated not solely  
262 with myocardial damage, but also with the depth at which the lead is positioned  
263 within the ventricular septum. If the COI does not increase when the electrode is  
264 initially inserted under the right septal imaging positioning, it implies that the  
265 electrode is entangled with the endometrium or myocardial fibrosis, necessitating a  
266 change in position. The peak of the ventricular COI is not observed in the left deep  
267 septum; rather, it is in the mid-interventricular septum where the maximum amplitude  
268 is recorded. Positioning of the lead in the mid-interventricular septum may suggest its  
269 optimal stability.

270 Evidence from previous studies indicates that IVSP is characterized by a relatively  
271 short RWPT and QRS duration, indicative of a superior level of synchronicity  
272 between the left and right ventricles associated with this pacing modality. Our  
273 research also suggests the potential for this modality to offer superior stability.  
274 Consequently, given the current lack of consensus regarding the optimal strategy for  
275 trans-septal pacing, IVSP may be considered a viable choice for practitioners seeking  
276 to attain the greatest lead stability and good ventricular synchrony. Compared to  
277 left-side deep septal pacing (including LVSP and LBBP), the application of IVSP  
278 may be more straightforward and presents a lower risk of perforation.

279

280 **Deep septal pacing lead localization and perforation**

281 The implantation technique of LBBP involves inserting a lead into the deep septum  
282 below the left ventricular subendocardium to engage the LBB. The number of  
283 rotations required to access the LBB area is dependent on factors such as septal  
284 thickness, the degree of fibrosis, and sheath support. The assessment of ventricular  
285 perforation can be conducted using X-ray fluoroscopy and echocardiography, but the  
286 precise positioning of the intramyocardial lead often remains unclear due to the lack  
287 of soft tissue visualization in X-ray fluoroscopy and off-axis imaging planes in  
288 echocardiography. Typically, lead position is determined through the observation of  
289 ECG changes, while perforation detection relies on monitoring impedance changes  
290 and threshold assessments. However, impedance values can be significantly  
291 influenced by the quality of tissue-electrode contact, which varies during rapid  
292 screwing, making it challenging to accurately respond to real-time impedance  
293 changes.[19] Consequently, delays might occur in identifying perforation via  
294 impedance and threshold evaluations.

295 Septal perforation could be associated with the operator's endeavor to achieve the best  
296 possible paced QRS morphology and the LBB capture. This highlights the clinical  
297 need for the precise localization of the lead. The ventricular COI, represented by the  
298 unfiltered intracardiac electrical signal detected at the lead's tip, can accurately  
299 measure the contact between the lead and myocardial tissue, suggesting its potential  
300 to subtly discern ventricular perforation. This sensitivity primarily arises since any  
301 disruption in the lead-myocardium contact is immediately mirrored in this  
302 measurement. However, the current intermittent recording technique, which requires  
303 disconnection during lead screwing, limits the widespread use of this indicator by  
304 eliminating the possibility of real-time tracking of dynamic intracardiac electrical  
305 signal changes. Consequently, it becomes impossible to definitively confirm the  
306 occurrence of perforation during this process. Confirmation can only be achieved

307 once reconnection between the pacing lead and the external PSA is established,  
308 undeniably prolonging the procedure and increasing the risk of complications.  
309 The continuous recording technique addresses these limitations. As demonstrated in  
310 our research, the amplitude of the ventricular COI allows for real-time determination  
311 of the radial depth of the lead within the interventricular septum, thereby facilitating  
312 the prevention and detection of perforations. During the entire screw-in process, it  
313 was observed that the amplitude of the ventricular COI increases and peaks as the lead  
314 is inserted from the right septum to the mid-septum. As the lead continues to be  
315 inserted deeper into the left septum, the ventricular COI amplitude gradually  
316 decreases, eventually approximating the amplitude initially detected within the right  
317 septum. In our study, it was observed that the ventricular COI from both the right and  
318 left septum were closely aligned. Consequently, it was inferred that by monitoring the  
319 COI of the right septum, the ventricular COI amplitude of the left septum could be  
320 predicted. This insight enabled us to determine, with greater precision, the  
321 individualized endpoint for halting the screwing into the left ventricular endocardium,  
322 based on the COI amplitude in the right ventricular septum. At this stage, the lead  
323 should be manipulated with care to prevent a sudden drop in the ventricular COI.  
324 Simultaneously, dynamic changes in the ECG, such as an abrupt shortening of  
325 V6RWPT and the emergence of an initial r wave in the V1 lead, need to be closely  
326 monitored. Once these changes are detected, the rotation of the lead should be  
327 immediately terminated and threshold testing conducted, typically revealing a discrete  
328 ventricular electrogram.  
329 Even in the face of complications such as ventricular perforation, the advantages of  
330 the continuous recording technique allow for the rapid detection of a sudden decrease  
331 in ventricular COI, enabling early termination of lead rotation and a change in the  
332 implantation location. Simultaneously, this process discerns the nature of the  
333 perforation. It enables differentiation between a micro-perforation, where the helix  
334 partially enters the left ventricle cavity, and a complete perforation, where the helix

335 fully penetrates the ventricular septum. With micro-perforations, the ventricular COI  
336 can still be observed, whereas complete perforations typically present as a QS  
337 pattern.[20]

338

### 339 **Selective left bundle branch pacing**

340 The gold standard for confirming LBB capture typically involves observing a  
341 transition in QRS morphology, a change that indicates differences in excitability (as  
342 measured by threshold testing) and/or refractoriness (as determined by programmed  
343 stimulation) between the LBB and myocardium.[11] Wu et al. demonstrated that an  
344 LBB potential can still be recorded by the lead even when positioned a certain  
345 distance away from the LBB, suggesting that the presence of an LBB potential does  
346 not necessarily confirm LBB capture.[21] A previous study proposed that the LBB  
347 COI reflects the anatomical location of the tip of the lead within the LBB region,  
348 possibly due to localized cell membrane damage caused by the pressure exerted by  
349 the electrode on the LBB. Therefore, recording an LBB potential with COI can serve  
350 as an indicator of LBB capture.[22] However, this method is only applicable to  
351 patients without left bundle branch block, as a considerable proportion of patients do  
352 not have  $P_{OLBB}$  and thereby LBB COI, and its applicability is somewhat limited.

353 As previous studies have shown, the presence of ventricular COI is associated with  
354 adequacy of lead fixation in the endocardium.[16-18] It is generally believed that  
355 ventricular COI itself is not diagnostic for LBB capture.[23] In our study, besides  
356 finding that the characteristics of COI vary at different septum depths, small and  
357 significant changes in ventricular COI can also be observed when the NSLBB  
358 transition to SLBB capture. Just as filtered electrograms can display discrete EGM,  
359 unfiltered electrograms can also display discrete ventricular COI. Previous research  
360 has shown that the physiological Purkinje activation was like distal to proximal  
361 activation of the ventricular component.[24] A discrete EGM in the pacing lead can  
362 be recorded because direct myocardial capture is absent and therefore ventricular

363 activation over the pacing lead occurs late following initial conduction only over the  
364 LBB-Purkinje system. Recording discrete EGM was defined as SLBBP and had a  
365 specificity of 100% for confirmation of LBB capture, which was demonstrated by a  
366 previous study.[25] Therefore, the discrete ventricular COI can also serve as an  
367 electrophysiological phenomenon for capturing the LBB.

368

### 369 **Conclusion**

370 In this study, we present a detailed description of the electrophysiological properties  
371 of unipolar lead-position-dependent EGM. Such insights offer clinicians a subtle  
372 understanding of the radial depth of the pacing lead throughout the implantation  
373 process. Given that IVSP results in the most favorable ventricular COI, this strategy  
374 provides operators with a more selection of pacing locations. Furthermore, the  
375 emergence of a discrete ventricular COI may serve as a novel characteristic of SLBBP.  
376 Consequently, the use of continuous recording technique enables the observation of a  
377 broader array of electrophysiological phenomena during traversal of the IVS. This  
378 approach not only provides practitioners with more insights but also simplifies  
379 implantation procedures and facilitates the prevention or early detection of  
380 perforations. Future studies are needed to further validate these findings and explore  
381 their clinical implications.

382

### 383 **Study Limitations**

384 This study has several limitations that should be noted. Firstly, the study was  
385 conducted at a single center, and the sample size was relatively small. This may limit  
386 the generalizability of our findings to broader populations or different clinical settings.  
387 Secondly, the observational nature of the study design precludes the determination of  
388 causality. Future studies with randomized controlled trials are needed to establish  
389 causal relationships between the variables we studied. Thirdly, we used specific  
390 equipment and techniques for the continuous recording of electrophysiological

391 phenomena during left bundle branch pacing. The results might not be applicable to  
392 centers using different types of equipment or techniques. Lastly, although our study  
393 provides evidence that the continuous recording technique can facilitate the  
394 observation of a broader array of electrophysiological phenomena during traversal of  
395 the IVS, more research is needed to determine whether this approach can improve  
396 clinical outcomes, such as reducing the incidence of complications or improving the  
397 long-term stability of the pacing lead.

398

#### 399 **Conflict of interest**

400 The corresponding author owns the patent for John Jiang's connecting cable. The  
401 other author declares no conflict of interest.

402

#### 403 **Funding Sources**

404 This work was supported by the Ningbo Public Service Technology Foundation [grant  
405 number 2023S089], Zhejiang Provincial Public Service and Application Research  
406 Foundation, China [grant number LGF22H020009], and Zhu Xiu Shan Talent Project  
407 of Ningbo No.2 Hospital, China [grant number 2023HMYQ18].

408

#### 409 **References**

- 410 1. Huang W, Su L, Wu S, et al. A Novel Pacing Strategy With Low and Stable  
411 Output: Pacing the Left Bundle Branch Immediately Beyond the Conduction  
412 Block. *Can J Cardiol* 2017, 33:1736.e1731-1736.e1733.
- 413 2. Mafi-Rad M, Luermans JGLM, Blaauw Y, et al. Feasibility and Acute  
414 Hemodynamic Effect of Left Ventricular Septal Pacing by Transvenous  
415 Approach Through the Interventricular Septum. *Circulation Arrhythmia and*  
416 *Electrophysiology* 2016, 9:e003344.

- 417 3. Jastrzębski M, Kielbasa G, Moskal P, et al. Fixation beats: A novel marker for  
418 reaching the left bundle branch area during deep septal lead implantation.  
419 Heart Rhythm 2021, 18:562-569.
- 420 4. Ponnusamy SS, Vijayaraman P. Left bundle branch pacing guided by  
421 premature ventricular complexes during implant. HeartRhythm Case Rep 2020,  
422 6:850-853.
- 423 5. Shen J, Jiang L, Cai X, et al. Left Bundle Branch Pacing Guided by  
424 Continuous Pacing Technique That Can Monitor Electrocardiograms and  
425 Electrograms in Real Time: A Technical Report. Can J Cardiol 2022,  
426 38:1315-1317.
- 427 6. Wu H, Jiang L, Shen J. Recording an isoelectric interval as an endpoint of left  
428 bundle branch pacing with continuous paced intracardiac electrogram  
429 monitoring. Kardiol Pol 2022, 80:664-671.
- 430 7. Shen J, Jiang L, Wu H, et al. A Continuous Pacing and Recording Technique  
431 for Differentiating Left Bundle Branch Pacing From Left Ventricular Septal  
432 Pacing: Electrophysiologic Evidence From an Inpatient-Controlled Study.  
433 Can J Cardiol 2023, 39:1-10.
- 434 8. Chen K, Li Y, Dai Y, et al. Comparison of electrocardiogram characteristics  
435 and pacing parameters between left bundle branch pacing and right ventricular  
436 pacing in patients receiving pacemaker therapy. Europace 2019, 21:673-680.
- 437 9. Jastrzębski M, Burri H, Kielbasa G, et al. The V6-V1 interpeak interval: a  
438 novel criterion for the diagnosis of left bundle branch capture. Europace 2022,  
439 24:40-47.
- 440 10. Shimeno K, Matsumoto N, Matsuo M, et al. Device Electrogram-Guided  
441 Determination of Output-Dependent QRS Transition in Left Bundle Branch  
442 Pacing. JACC Clin Electrophysiol 2024:102308.
- 443 11. Burri H, Jastrzebski M, Cano Ó, et al. EHRA clinical consensus statement on  
444 conduction system pacing implantation: endorsed by the Asia Pacific Heart



- 445 Rhythm Society (APHRs), Canadian Heart Rhythm Society (CHRS), and  
446 Latin American Heart Rhythm Society (LAHRS). *Europace* 2023,  
447 25:1208-1236.
- 448 12. Chung MK, Patton KK, Lau CP, et al. 2023 HRS/APHRs/LAHRS guideline  
449 on cardiac physiologic pacing for the avoidance and mitigation of heart failure.  
450 *Heart Rhythm*. 2023 Sep;20(9):e17-e91.
- 451 13. Liu X, Niu HX, Gu M, et al. Contrast-enhanced image-guided lead  
452 deployment for left bundle branch pacing. *Heart Rhythm*. 2021  
453 Aug;18(8):1318-1325.
- 454 14. Shen J, Jiang L, Wu H, et al. High-pass filter settings and the role and  
455 mechanism of discrete ventricular electrograms in left bundle branch pacing.  
456 *Front Cardiovasc Med* 2022, 9:1059172.
- 457 15. Shen J, Jiang L, Wu H, et al. Left bundle branch pacing guided by real-time  
458 monitoring of current of injury and electrocardiography. *Front Cardiovasc*  
459 *Med* 2022, 9:1025620.
- 460 16. Saxonhouse SJ, Conti JB, Curtis AB. Current of injury predicts adequate  
461 active lead fixation in permanent pacemaker/defibrillation leads. *J Am Coll*  
462 *Cardiol* 2005, 45:412-417.
- 463 17. Redfearn DP, Gula LJ, Krahn AD, et al. Current of injury predicts acute  
464 performance of catheter-delivered active fixation pacing leads. *Pacing Clin*  
465 *Electrophysiol* 2007, 30:1438-1444.
- 466 18. Haghjoo M, Mollazadeh R, Aslani A, et al. Prediction of midterm  
467 performance of active-fixation leads using current of injury. *Pacing Clin*  
468 *Electrophysiol* 2014, 37:231-236.
- 469 19. Jastrzębski M. Left bundle branch area pacing lead implantation using an  
470 uninterrupted monitoring of endocardial signals. *J Cardiovasc Electrophysiol*.  
471 2022 May;33(5):1055-1057.

- 472 20. Ponnusamy SS, Basil W, Vijayaraman P. Electrophysiological characteristics  
473 of septal perforation during left bundle branch pacing. *Heart Rhythm*. 2022  
474 May;19(5):728-734.
- 475 21. Wu H, Jiang L, Shen J. Characteristics and proposed meaning of intrinsic  
476 intracardiac electrogram morphology observed during the left bundle branch  
477 pacing procedure: A case report. *HeartRhythm Case Rep* 2022, 8:485-487.
- 478 22. Su L, Xu T, Cai M, et al. Electrophysiological characteristics and clinical  
479 values of left bundle branch current of injury in left bundle branch pacing. *J*  
480 *Cardiovasc Electrophysiol* 2020, 31:834-842.
- 481 23. Shali S, Wu W, Bai J, et al. Current of injury is an indicator of lead depth and  
482 performance during left bundle branch pacing lead implantation. *Heart*  
483 *Rhythm*. 2022 Aug;19(8):1281-1288.
- 484 24. Upadhyay GA, Cherian T, Shatz DY, et al. Intracardiac Delineation of Septal  
485 Conduction in Left Bundle-Branch Block Patterns. *Circulation* 2019,  
486 139:1876-1888.
- 487 25. Wu S, Chen X, Wang S, et al. Evaluation of the Criteria to Distinguish Left  
488 Bundle Branch Pacing From Left Ventricular Septal Pacing. *JACC Clin*  
489 *Electrophysiol* 2021, 7:1166-1177.

490

#### 491 **Figure legends**

492 **Figure 1** The procedure to implant the LBBP lead under fluoroscopy. A.  
493 Visualization of the TVA to help locate the LBBP target zone under the RAO 30°  
494 view. B-C. The 3830 lead was positioned in the LBBP screw-in site and fixed site  
495 under the RAO 30° view. D-F. Through the combination of septal angiography and  
496 the paced ECG and EGM morphologies associated, the RVSP, IVSP, and LBBP was  
497 confirmed. RAO, right anterior oblique; TVA, tricuspid valve annulus; RVSP, right  
498 ventricular septal pacing; IVSP, intraventricular septal pacing; LBBP, left bundle  
499 branch pacing; ECG, electrocardiogram; EGM, intracardiac electrogram.

500

501 **Figure 2** Lead-position-dependent EGM and ECG transition during screwing in.  
502 NSLBBP, nonselective left bundle branch pacing; SLBBP, selective left bundle  
503 branch pacing; LBB-F, filtered unipolar electrogram; LBB-U, unfiltered unipolar  
504 electrogram.

505

506 **Figure 3** Electrophysiological characteristics of EGM and ECG in 5 pacing patterns.  
507 COI, current of injury; Stim-V6RWPT, stimulus to V6 R-wave peak time;  
508 Stim-V1RWPT, stimulus to V1 R-wave peak time. Abbreviations as in Figure 1 and  
509 2.

510

511 **Figure 4** Discrete COI can be observed when the NSLBBP transition to SLBBP  
512 during threshold testing. Hollow arrows are used to indicate the appearance of notches.  
513 Abbreviations as in Figure 1 and 2.

514

515 **Figure 5** The continuous recording technique enables real-time monitoring of the  
516 entire perforation process, facilitating early detection of perforations. The impedance  
517 can be observed to drop from 662  $\Omega$  to 501  $\Omega$ . Abbreviations as in Figure 2.

518

519

520

521

522

523

524

525

526

527

528  
529  
530  
531  
532  
533  
534  
535  
536  
537  
538

**Table 1. Patient characteristics (n = 88)**

Age (years)	73.7 ± 9.1
Male	51 (58.0)
Pacing indication, n (%)	
Atrioventricular block	56 (63.6)
Sick sinus syndrome	31 (35.2)
Atrial fibrillation with bradycardia	4 (4.5)
Heart failure	5 (5.7)
Comorbidities, n (%)	
Hypertension	53 (60.2)
Diabetes mellitus	23 (26.1)
Cardiomyopathy	4 (4.5)
Coronary heart disease	14 (16.0)
Atrial fibrillation	22 (25.0)
LVEF (%)	62.8 ± 11.1
LVDD (mm)	49.7 ± 7.8
QRS morphology, n (%)	
Narrow QRS	60 (68.2)
RBBB	19 (21.6)
LBBB	11 (12.5)
NIVCD	2 (2.3)

Values are given as mean ± SD or n (%).

LVEF, left ventricular ejection fraction; LVDD, left ventricular end-diastolic dimension; RBBB, right bundle branch block; LBBB, left bundle branch block; NIVCD, non-specific intraventricular conduction disturbance.

539  
540  
541  
542  
543  
544  
545  
546  
547  
548  
549

**Table 2. Procedure-related parameters (n=88)**

Incidence of P <sub>OLBB</sub> , n (%)	66 (75.0%)
P <sub>OLBB</sub> -ventricular interval, ms	24.7 ± 8.1
P <sub>OLBB</sub> -V6RWPT, ms	64.5 ± 7.1
P <sub>OLBB</sub> amplitude, mV	0.35 ± 0.34
Abrupt shortening of stim-V6RWPT, ms	14.0 ± 5.9
Initial LBB capture threshold, V/0.5 ms	0.76 ± 0.56
Initial LVS capture threshold, V/0.5 ms	1.32 ± 0.91
Initial R-wave amplitude, mV	8.1 ± 3.9
Initial Impedance, Ω	783.6 ± 145.9
Final LBB capture threshold, V/0.5 ms	0.61 ± 0.44
Final LVS capture threshold, V/0.5 ms	0.66 ± 0.25
Final R-wave amplitude, mV	15.1 ± 7.1
Final Impedance, Ω	743.1 ± 136.8
Lead depth, mm	15.1 ± 2.6
Perforation, n (%)	3 (3.4%)

Values are given as mean ± SD or n (%). P<sub>OLBB</sub>, left bundle branch potential; stim-V6RWPT, stimulus to V6 R wave peak time; LVS, left ventricular septal.

550  
551  
552  
553  
554

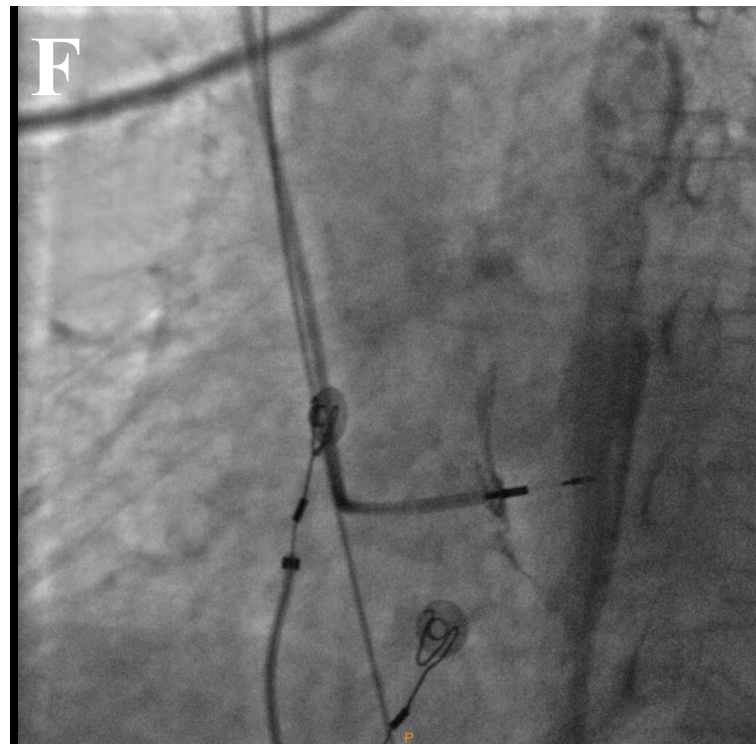
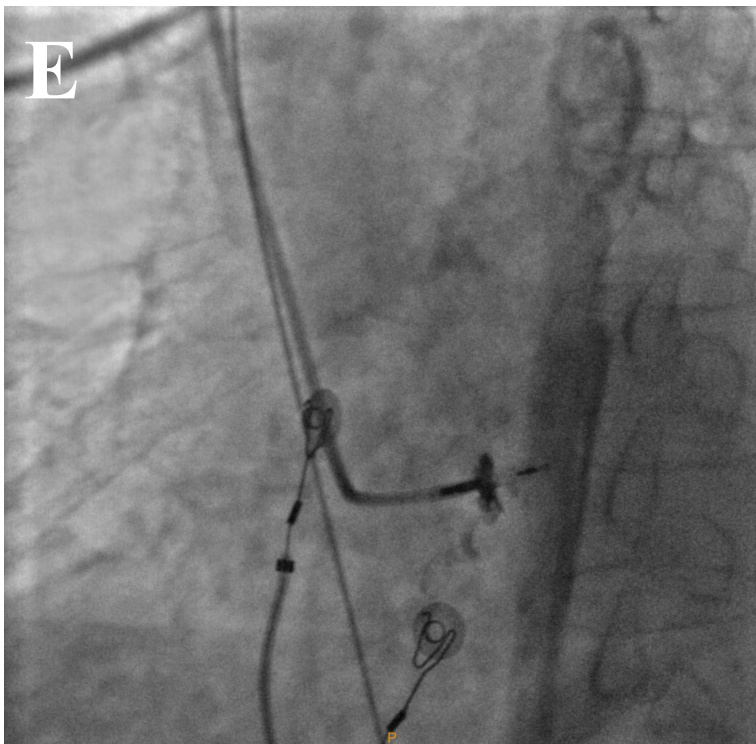
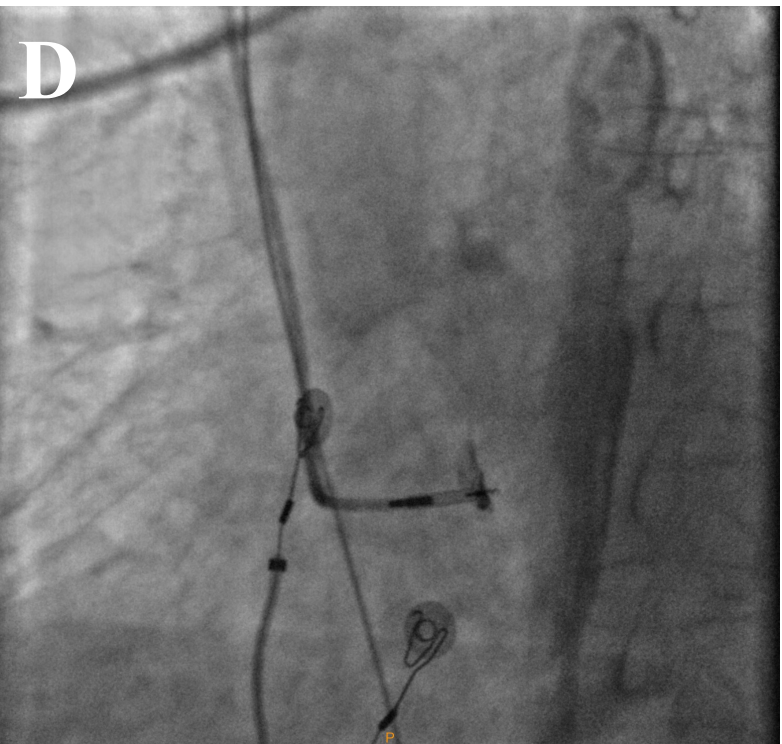
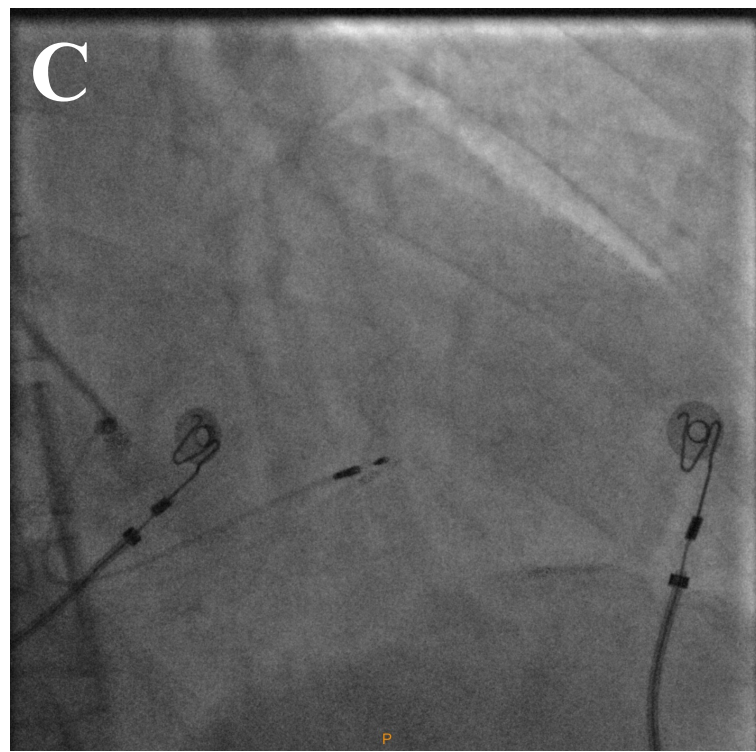
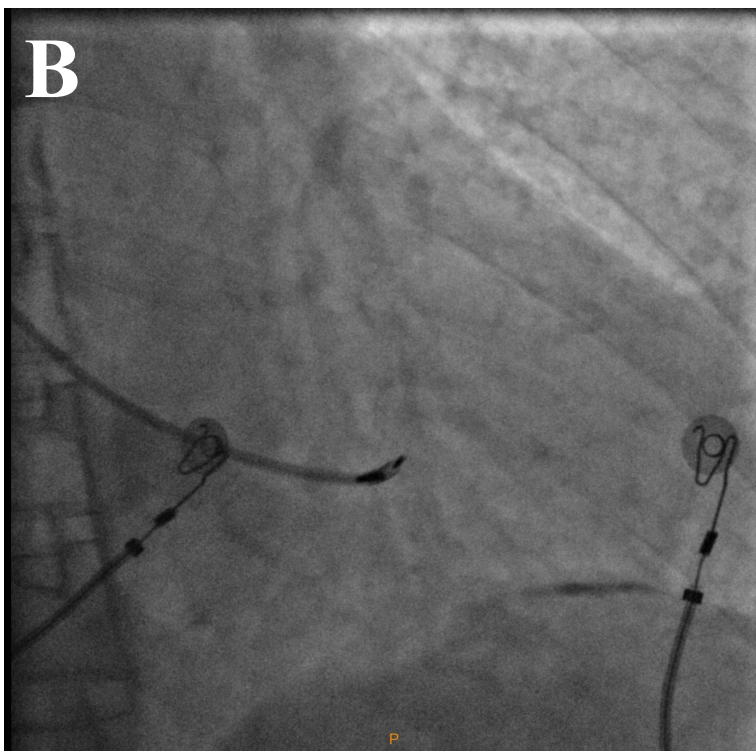
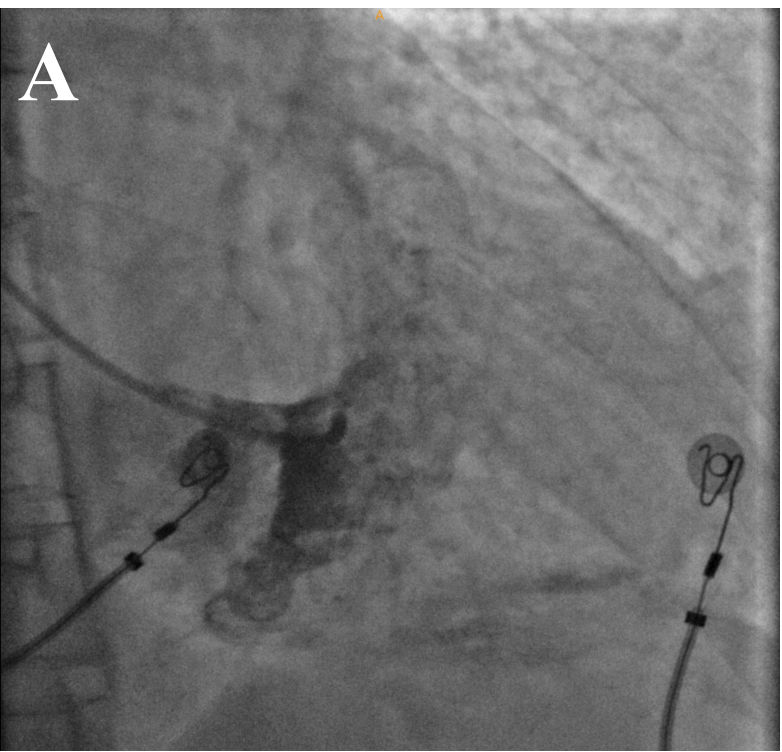
555  
556  
557  
558  
559  
560  
561  
562  
563  
564  
565

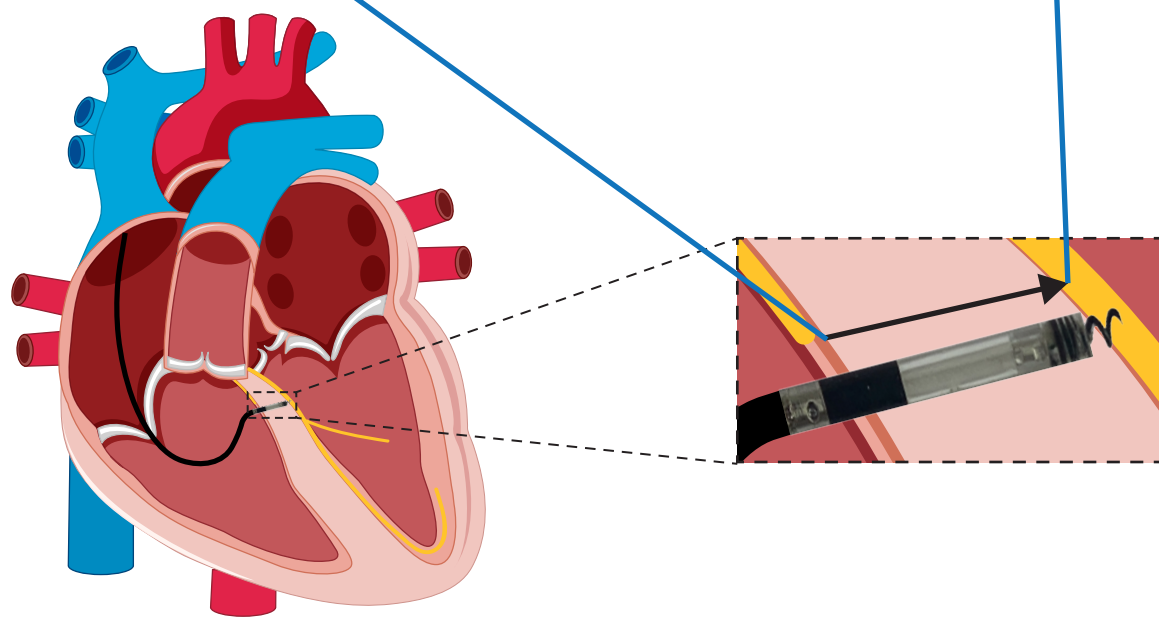
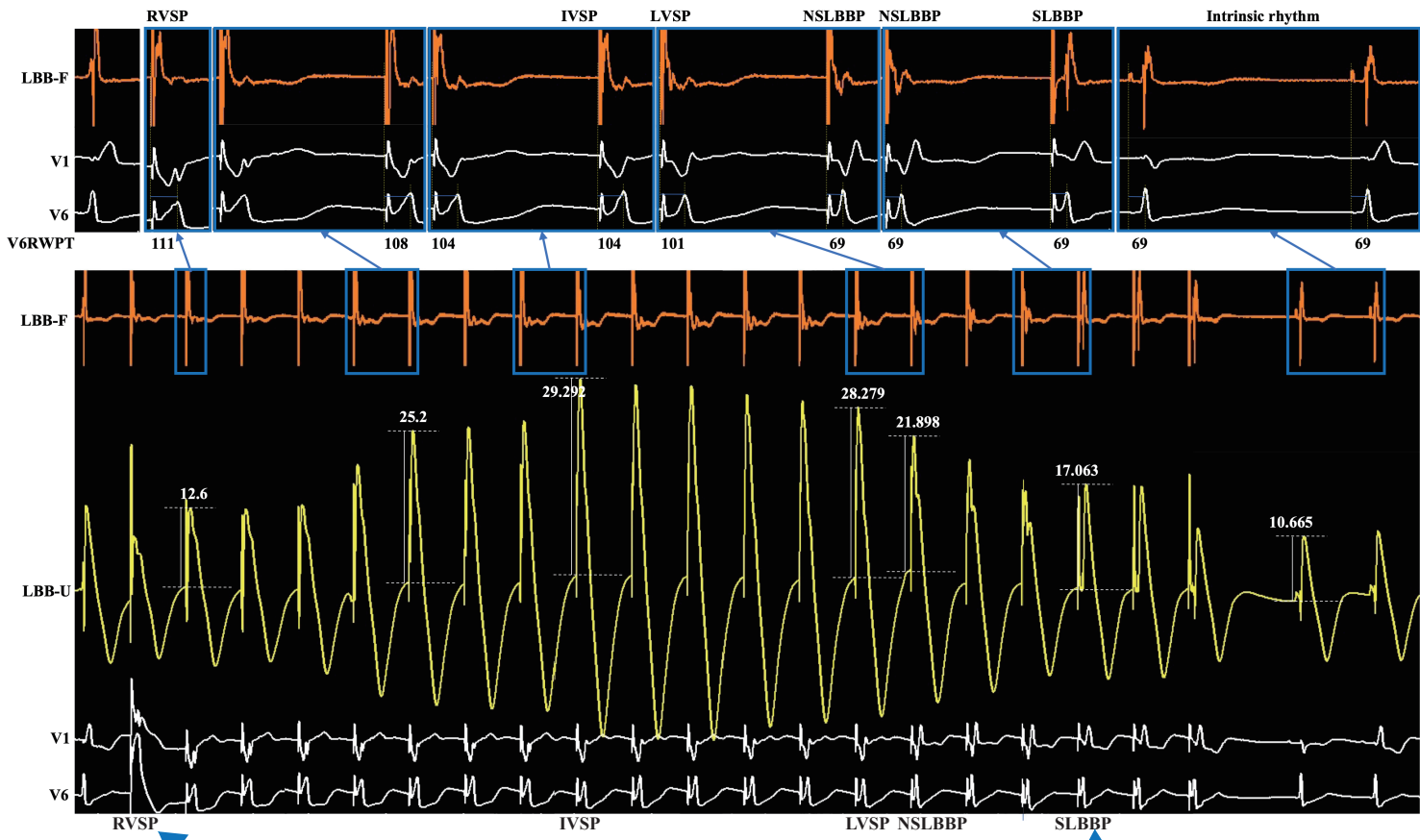
**Table 3. Lead-position–dependent parameters during LBBP**

	RVSP	IVSP	LVSP	NSLBBP	SLBBP	Pre-pac impla
COI (mV)	10.5±5.9	26.6±11.8	19.8±9.6	20.0±9.2	11.9±6.4	
Impedance (Ω)	948.7±202.1	980.3±156.3	NA	929.5±191.4	886.0±164.4	743.1
Stim-V6RWPT (ms)	103.2±16.9	83.8±12.5	81.8±12.3	67.5±9.7	66.9±9.5	70.
Stim-V1RWPT (ms)	NA	105.8±12.0	113.7±11.0	110.4±12.1	118.4±16.1	114.
Stim-QRSend (ms)	148.0±14.9	133.9±13.8	138.6±14.3	136.0±18.8	147.5±17.6	144.

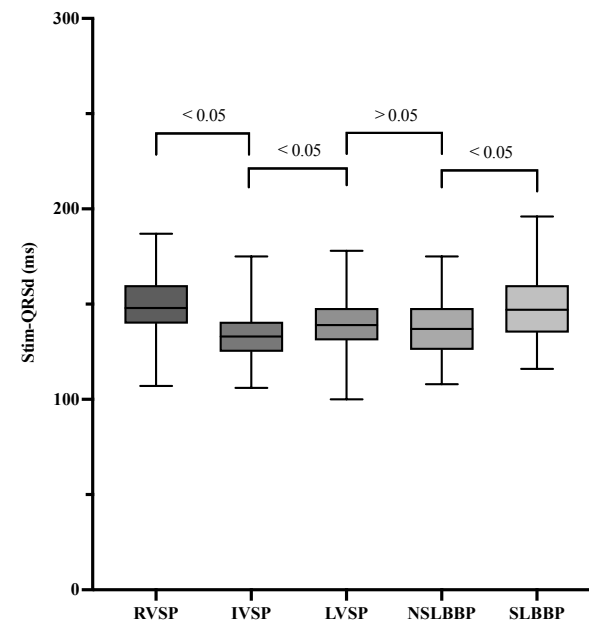
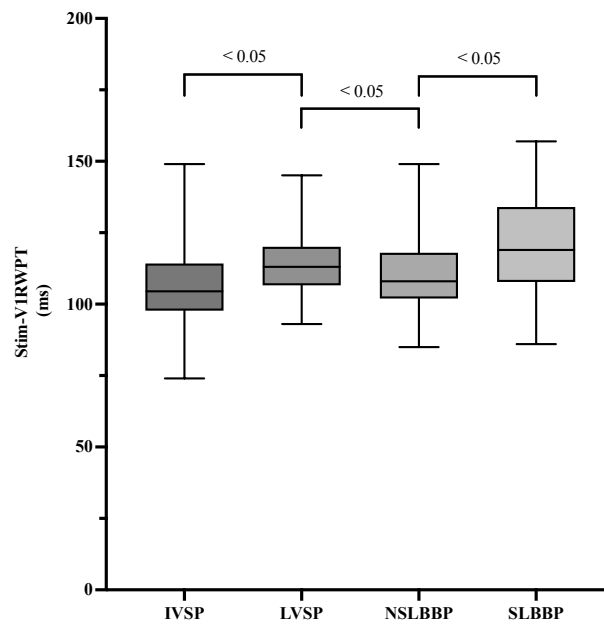
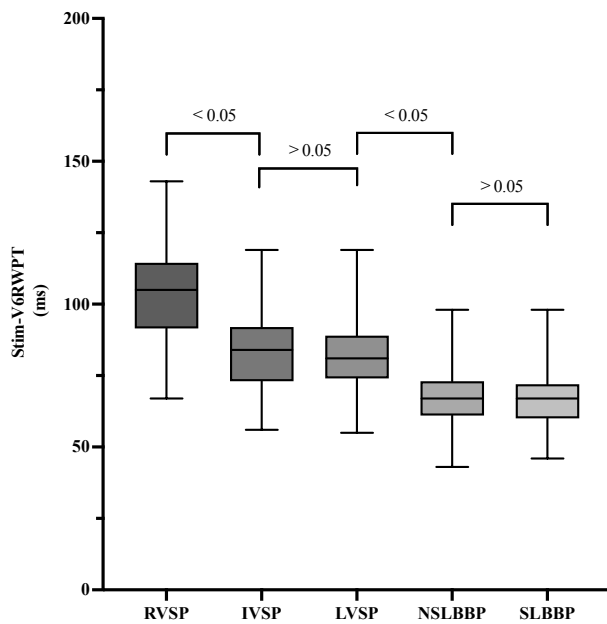
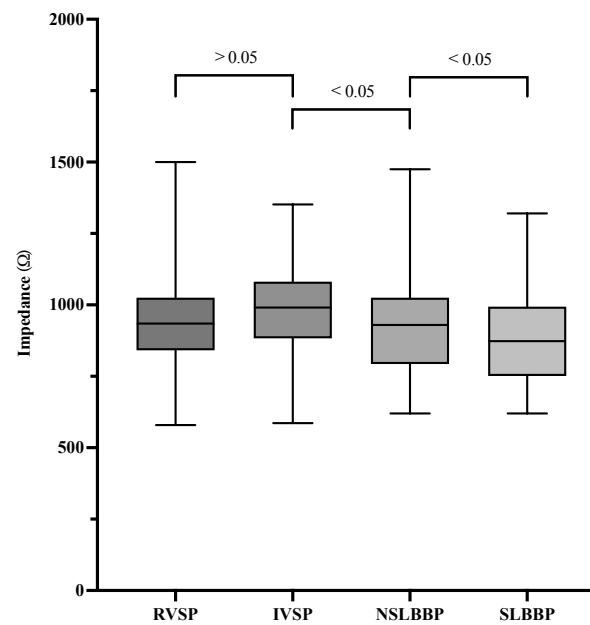
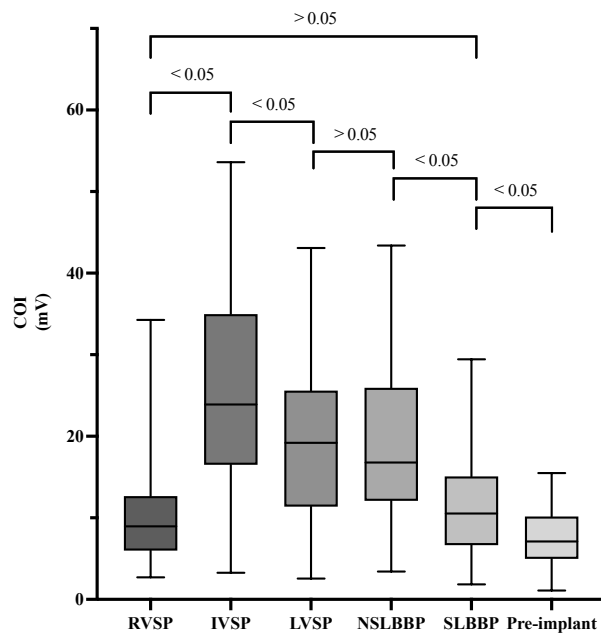
RVSP, right ventricular septal pacing; IVSP, intraventricular septal pacing; LVSP, left ventricular septal endocardium pacing; NSLBBP, non-selective left bundle branch pacing; SLBBP, selective left bundle branch pacing; COI, current of injury; RWPT, R wave peak time; Stim-QRSend, stimulus-QRS end duration.

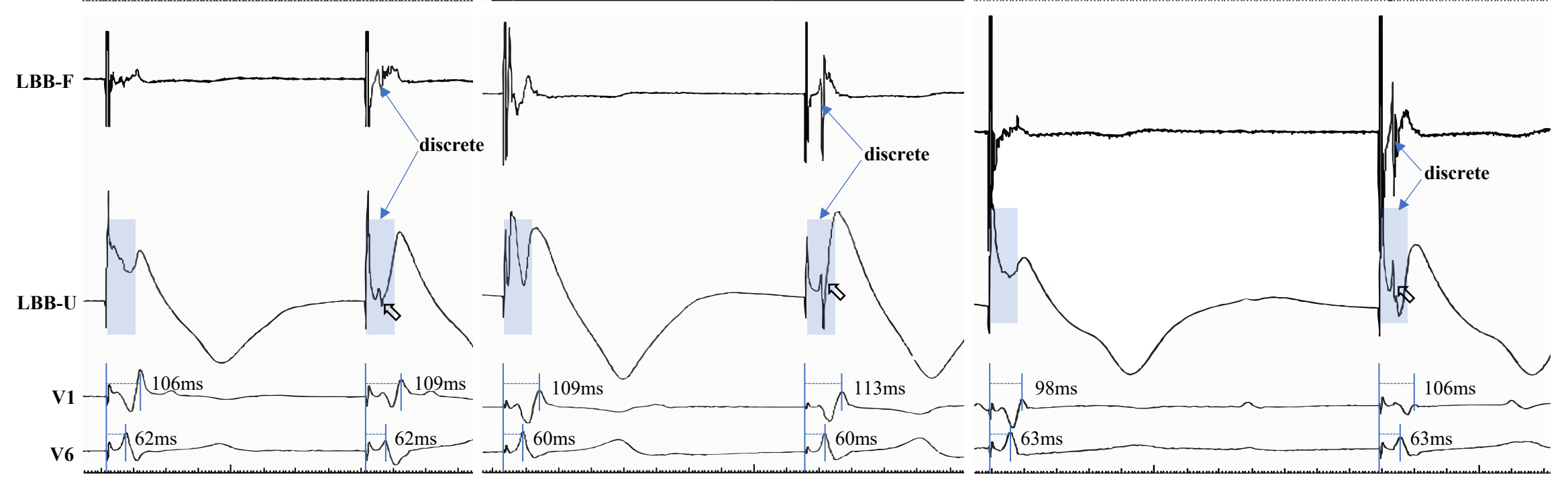
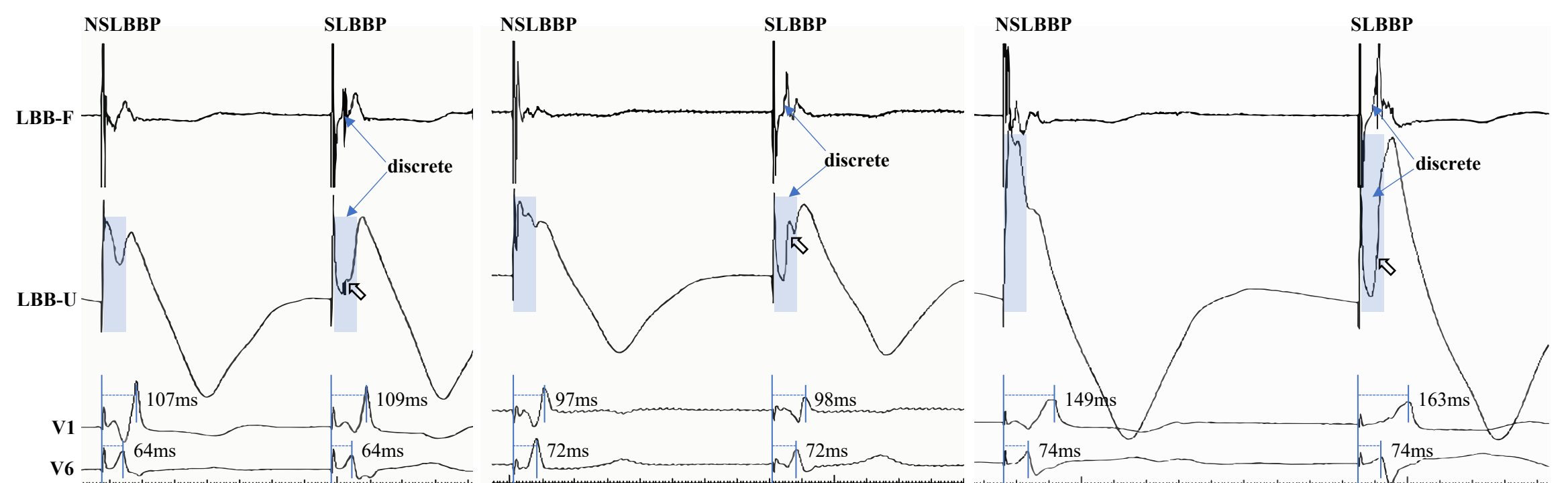
566











662

perforation

501

Loss capture

LBB-F

LBB-U

